Korean J. Chem. Eng., **28**(2), 620-626 (2011)
DOI: 10.1007/s11814-010-0373-6

Polylactic acid/epoxidized palm oil/fatty nitrogen compounds modified clay nanocomposites: Preparation and characterization

Emad Abbas Jaffar Al-Mulla†

Department of Chemistry, College of Science, University of Kufa, AnNajaf, Iraq
(*Received 28 March 2010 • accepted 7 July 2010*)

Abstract−Clay modification was carried out by treatment of fatty nitrogen compounds (FNCs); fatty hydrazide (FH), hydroxy methyl fattyamide (HMFA), and difatty acyl thiourea (DFAT) were synthesized from vegetable oils with a sodium montmorillonite (MMT) as natural clay. This process was accomplished by stirring the clay particles in an aqueous solution of FH, HMFA, and DFAT, by which the clay layer thickness increased from 1.23 to 2.69, 2.89 and 3.21 nm, respectively. The modified clay was then used in the preparation of the polylactic acid/epoxidized palm oil (PLA/EPO) blend nanocomposites. The interaction of the modifier in the clay layer was characterized by X-ray diffraction (XRD) and Fourier transform infrared (FTIR). Elemental analysis was used to estimate the presence of FNCs in the clay. The nanocomposites were synthesized by solution casting of the modified clay and a PLA/EPO blend at the weight ratio of 80/20, which has the highest elongation at break. The nanocomposites were then characterized using XRD, transmission electron microscopy (TEM), thermogravimetric analysis (TGA), and tensile properties measurements. Improvement in mechanical properties of the FH-MMT, HMFA-MMT, and DFAT-MMT nanocomposites was obtained when 2% of the DFAT-MMT and 3% of both FH-MMT and HMFA-MMT loadings were used. PLA/EPO modified clay nanocomposites show higher thermal stability in comparison with those of the PLA/EPO blend. The XRD and TEM results confirmed the production of nanocomposites.

Key words: Nanocomposites, Montmorillonite, FNCs, Epoxidized Palm Oil

INTRODUCTION

Biodegradable polyesters have attracted much attention due to their biodegradability and biocompatibility which offer clear advantages for both customers and environment.

One of the most promising candidates for biodegradable synthetic polyesters is PLA [1]. PLA can be obtained from renewable resources by means of a fermentation process using sugar from corn, either by ring-opening polymerization or by condensation polymerization. It is a linear aliphatic thermoplastic polyester that is readily biodegradable by enzyme action [2].

In addition to its application in the textile industries, automotive and clinical uses, PLA represents a good candidate to produce disposable packaging because of its good mechanical properties and processability [3,4]. However, a high tensile, a high modulus, low elongation at break and a high price limit its application. Therefore, the tailoring of its properties to reach end-user demands is required.

Attempts have been made to enhance the flexibility and other mechanical properties by the blending of PLA with other polymers such as polycaprolactone, polybutylene succinate or polyetherurethane [5,6]. Low molecular weight plasticizers such as polyethylene glycol, polypropylene glycol and citrate esters were also used to improve the thermal and mechanical properties of PLA [7,8].

The incorporation of organoclays in the polymer to produce a nanocomposite is another means to modify the property balance of a material. The improvements in thermal stability, physical and mechanical properties can be achieved by addition of 2-5 percent weight of organoclays in comparison to the neat polymer [9-11].

The modification of natural clay (montmorillonite) may be carried out via exchanging the original inter-layer cations by organic cations where they are transformed from organophobic to organophilic materials and significantly increase the basal spacing of the clay layers [12]. It is generally accepted that the extent of swelling depends on the length of the alkyl chain and the cation exchange capacity of the clay [20]. Organoclays are mainly obtained by exchanging cations in the clay minerals, which contain hydrated Na^+ ions with alkylammonium [21].

Processing and properties of PLA/thermoplastic starch/montmorillonite nanocomposites were investigated and characterized using X-Ray diffraction, transmission electron microscopy and tensile measurements. The results show improvement in the tensile modulus and strength and a reduction in fracture toughness [22].

Plasticized PLA-based nanocomposites were prepared and characterized with polyethylene glycol and montmorillonite. It is reported that the organo-modified montmorillonite-based composites have shown the possible competition between the polymer matrix and the plasticizer for the intercalation between the alumino-silicate layers [23].

In this study, fatty nitrogen compounds (FNCs) synthesized from vegetable oil were used for modification of the montmorillonite. The presence of long-chain fatty acids (mainly 16 and 18 carbon atoms) in FNCs containing O and N donor sets suggests FNCs should be very useful as surfactants for clay modification. The use of FNCs reduces the dependence on petroleum-based surfactants. The present study shows plasticized PLA-based nanocomposites with epoxi-

†To whom correspondence should be addressed.
E-mail: emadaalmulla@yahoo.com

dized palm oil (EPO) and montmorillonite modified by DNCs. EPO is an epoxidized derivative of a mixture of esters of glycerol with various saturated and unsaturated fatty acids. This is important for many chemical industries as they are derived from renewable, biodegradable, environmentally friendly and easily available raw materials.

EXPERIMENTAL

1. Materials

Epoxidized palm oil was obtained from AOTD, Malaysia. Sodium montmorillonite (Kunipia F) was obtained from Kunimine Ind. Co., Japan. Polylactic acid and chloroform were from T.J.Baker, USA and Merck, Germany, respectively.

2. Preparation of Organoclay

Organoclay was prepared with a cationic exchange process, where Na^+ in the montmorillonite was exchanged with alkylammonium ion from FNCs synthesized from triacylglycerides, which were reported in our previous papers [24-26], in an aqueous solution. 4.00 g of sodium montmorillonite (Na-MMT) was stirred vigorously in 600 ml of hot distilled water for 1 hour to form a clay suspension. Subsequently, a designated amount of fatty nitrogen compounds, which had been dissolved in 400 ml of hot water and the desired amount of concentrated hydrochloric acid (HCl) was added into the clay suspension of fatty nitrogen compounds. After being stirred vigorously for 1 hour at 80 °C, the organoclay suspension was filtered and washed with distilled water until no chloride was detected with a 1.0 M silver nitrate solution. It was then dried at 60 °C for 72 hours. The dried organoclay was ground until the particle size was less than 100 μm before the preparation of the nanocomposite. The amounts of hydrochloric acid, and FNCs used in this study are listed in Table 1.

Table 1 The optimization of basal spacing of modified montmorillonite with different amounts of fatty nitrogen compounds and hydrochloric acid

Amount of FNCs (g) in 4.00 g of MMT	Conc. HCl (mL)	d-Spacing (nm)		
		FH-MMT	HMFA-MMT	DFAT-MMT
1.00	4.00	1.27	1.31	1.58
1.50	4.00	1.29	1.38	1.75
2.00	4.00	1.32	1.42	1.84
2.50	4.00	1.47	1.53	1.90
3.00	4.00	1.49	1.61	2.01
3.50	4.00	1.51	1.66	2.11
4.00	4.00	1.54	1.71	2.19
4.50	4.00	1.61	1.80	2.25
5.00	4.00	1.63	1.84	2.31
4.50	6.00	1.70	2.02	2.47
4.50	8.00	1.86	2.27	2.57
4.50	10.00	2.02	2.48	2.71
4.50	12.00	2.13	2.62	2.90
4.50	14.00	2.40	2.75	3.11
4.50	16.00	2.68	2.87	3.20
4.50	18.00	2.70	2.90	3.21

Table 2 The amounts of PLA, EPO and modified clay in the nanocomposites

Sample identity	Weight of PLA (g)	Weight of EPO (g)	Weight of organoclay (g)
8PLA 2EPO	4.00	1.00	0.00
8PLA 2EPO mod1	3.96	0.99	0.05
8PLA 2EPO mod2	3.92	0.98	0.10
8PLA 2EPO mod3	3.88	0.97	0.15
8PLA 2EPO mod4	3.84	0.96	0.20
8PLA 2EPO mod5	3.80	0.95	0.25

mod1, mod2, mod3, mod4 and mod5=1%, 2%, 3%, 4% and 5% weight of organoclay, respectively

3. Preparation of PLA/EPO-clay Nanocomposites

The required amounts of PLA and EPO were dissolved in 50 ml of chloroform, separately. The EPO solution was then transferred into the PLA solution with a dropper and continuous stirring. After all the EPO solution was transferred into the PLA solution, the resultant mixture was then stirred for 1 hour. The required modified clay (FNCs-MMT) was then added into the dissolved PLA/EPO in the small portion. The mixture was then refluxed for 1 hour and then ultrasonically stirred using the Ultra Sonic Cathode for 10 minutes to make sure that the clay was fully dispersed in the PLA/EPO solution. The nanocomposite was then poured into a Petri dish and left to dry. The amount of PLA/EPO and the modified clay used in this study is listed in Table 2.

4. Characterization

4-1. X-ray Diffraction (XRD) Analysis

X-ray Diffraction (XRD) study was carried out using a Shimadzu XRD 6000 diffractometer with Cu-Kα radiation (λ=0.15406 nm). The diffractogram was scanned in the ranges from 2-10° at a scan rate of 1°/min.

4-2. Fourier Transform Infrared (FTIR)

The FTIR spectra of the samples were recorded by the FTIR spectrophotometer (Perkin Elmer FT-IR-Spectrum BX, USA) using the KBr disc technique.

4-3. Elemental Analysis

An elemental analyzer (LEO CHNS-932) was used for quantitative analysis of nitrogen contents in the organoclay. The determination was carried out under N_2 atmospheric conditions using sulfamethazine as a standard.

4-4. Thermogravimetric Analysis (TGA)

The thermal stability of the samples was studied by using the Perkin Elmer model TGA 7 Thermogravimetric Analyzer. The samples were heated from 35 to 800 °C with a heating rate of 10 °C/min under a nitrogen atmosphere with a nitrogen flow rate of 20 ml/min.

4-5. Tensile Properties Measurements

The tensile strength, tensile modulus and elongation at break were measured by using the Instron Universal Testing Machine 4301 at 5 mm/min of crosshead speed in accordance to ASTMD638 [27]. Seven samples were used for the tensile test and the average of five results was taken as the resultant value.

4-6. Transmission Electron Microscopy (TEM)

The dispersion of clay was studied by using energy filtering transmission electron microscopy (EFTEM). TEM pictures were taken

in a LEO 912 AB energy filtering transmission electron microscope with an acceleration voltage of 120 KeV. The specimens were prepared using an Ultracut E (Reichert and Jung) cryomicrotome. Thin sections of about 100 nm were cut with a diamond knife at −120 °C.

RESULTS AND DISCUSSION

Our results in a recent paper show that the PLA/EPO blend at a weight ratio of 80/20 has the highest elongation at break [28]. Therefore, this ratio was used in the subsequent experiments.

Fig. 1 shows the effect of clay content on the tensile properties of PLA/EPO/Na-MMT microcomposites, PLA/EPO/DFAT-MMT, PLA/EPO/FH-MMT, and PLA/EPO/HMFA-MMT nanocomposites. The reinforcing effect of unmodified montmorillonite in the PLA/EPO matrix was increased with a low increment rate. The maximum tensile strength was obtained when the clay content was 2% of the weight. Further increase of the clay content decreases tensile strength. Ma-MMT acts as a conventional particulate filler in the PLA/EPO matrix. Low tensile strength is obtained for PLA/EPO/

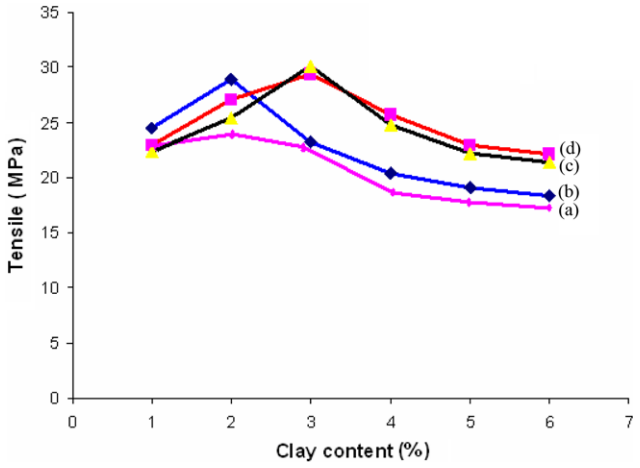

Fig. 1. Effect of clay content on the tensile strength of (a) PLA/EPO/ Na-MMT, (b) PLA/EPO/ DFAT-MMT, (c) PLA/EPO/FH-MMT, and (d) PLA/EPO/HMFA-MMT nanocomposites.

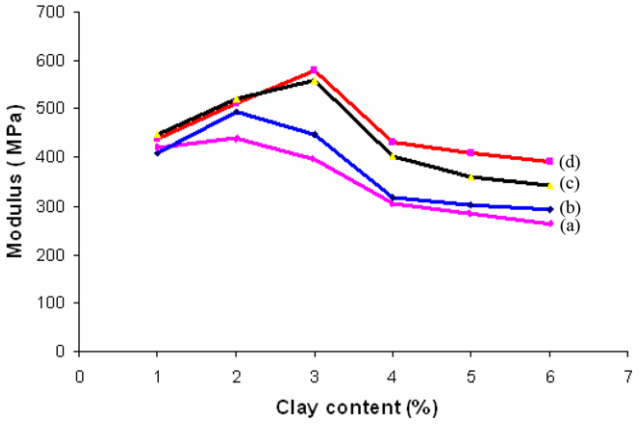

Fig. 2. Tensile modulus of (a) PLA/EPO/Na-MMT, (b) PLA/EPO/ DFAT-MMT, and (c) PLA/EPO/FH-MMT, and (d) PLA/EPO/ HMFA-MMT nanocomposites.

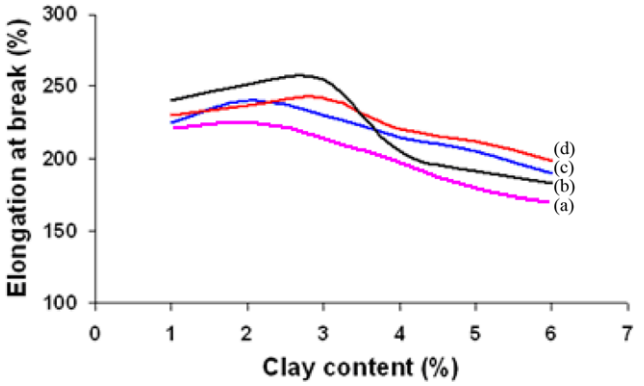

Fig. 3. Elangotion at break of (a) PLA/EPO/Na-MMT, (b) PLA/EPO/FH-MMT, (c) PLA/EPO/DFAT-MMT, and (d) PLA/EPO/ HMFA-MMT nanocomposites.

Na-MMT because the clay-clay interactions are stronger than that of the PLA/EPO-clay interactions [29]. A poor compatibility between the clay and PLA/EPO matrix is expected as the mixing is at a micro level [30]. A similar behavior of the clay content effect on the modulus and elongation at break of PLA/EPO/Na-MMT is observed (Figs. 2 and 3).

The increment of tensile strength, modulus, and elongation at break for the nanocomposites with FH-MMT, HMFA-MMT, and DFAT-MMT loadings are similar to that of the microcomposites. However, the rate of the increment of tensile properties for the nanocomposites increased.

The highest tensile strength, modulus, and elongation at break of the FH-MMT, HMFA-MMT, and DFAT-MMT nanocomposites were obtained when 3% of the FH-MMT or the HMFA-MMT and 2% of the DFAT-MMT loadings was used (Figs. 1-3). The enhancing effect of the FH-MMT, HMFA-MMT, and DFAT-MMT on the mechanical properties is probably due to the increase of the amount of the incorporated PLA/EPO chains in the clay layers. The polymer-clay interactions include the interactions of the intercalated PLA/EPO chains with the surface layers of the silicates. However, the tensile strength modulus, and elongation at break decrease when the FH-MMT, HMFA-MMT, and DFAT-MMT loadings are increased to more than 2% and 3% of FH-MMT and HMFA-MMT, and DFAT-MMT, respectively. The decrease of tensile strength, modulus, and elongation at break is due to the decrease of the PLA/EPO chains interacting with the clay as the clay coagglomerates.

According to Bragg's law ($n\lambda=d\sin\theta$), d refers to the distance of two consecutive clay layers, where λ is the wavelength of the intercept X-rays at the incident angle θ.

The presence of FNC chains in the galleries turns the original hydrophilic silicate to an organophilic silicate, and thus increases the layer-to-layer spacing of Na-MMT [17]. By using X-ray diffraction, Na-MMT shows a d001 diffraction peak at $2\theta=7.21^{\circ}$, which assigns the interlayer distance of the natural montmorillonite with a basal spacing of 1.23 nm. Na-MMT was surface treated with FNC as an intercalation agent through a cation exchange process. The cationic head groups of the intercalation agent molecule would preferentially reside at the surface layer and the aliphatic tail will radiate a ways from the surface.

The optimum amount of FNCs and HCl to reach maximum d-

Table 3. Diffraction angle and basal spacing of natural clay (Na-MMT) and modified clays with the FH-MMT, HMFA-MMT and DFAT-MMT

Sample	Exchanged cation	2 Theta (degree)	d-Spacing (nm)
Na-MMT	Na^+	7.21	1.23
FH-MMT	$RCONH\text{-}N^+H_3$	3.27	2.68
HMFA-MMT	$RCO\text{-}N^+HOH$ CH_3	3.05	2.87
DFAT-MMT	$(RCO)_2\ NHCSN^+H_2$	2.73	3.20

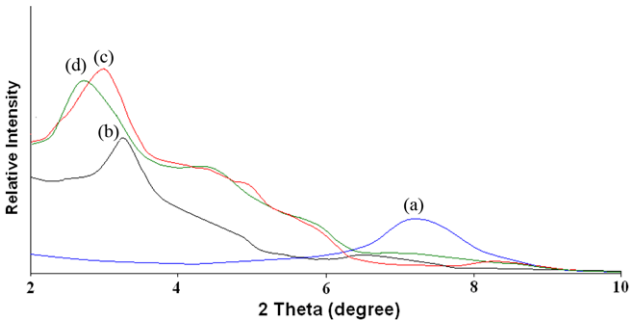

Fig. 4. XRD patterns of (a) Na-MMT, (b) FH-MMT, (c) HMFA-MMT, and (d) DFAT-MMT.

spacing was studied. It was found that the maximum d-spacing was achieved when the amount of FNC and HCl was 4.50 g and 16 mL, respectively (Table 1). There was no significant increase in d-spacing with a further increase in FNCs and HCl. The maximum basal spacing of FH-MMT, HMFA-MMT, and DFAT-MMT increases from 1.23 to 2.68, 2.87 and 3.20 nm, respectively (Table 3), indicating that these FNCs were successfully intercalated into the Na-MMT galleries (Fig. 4).

Greater basal spacing is observed for the DFAT-MMT than that of the HMFA-MMT and FH-MMT, suggesting that DFAT adopts a paraffin arrangement in the silicate layer, while a monolayer arrangement of HMFA and FH molecules is formed in the interlayer spacing of Na-MMT [31].

Fig. 5 shows the XRD patterns of the nanocomposites prepared using three different FNC (alkylammonium groups) modified mont-

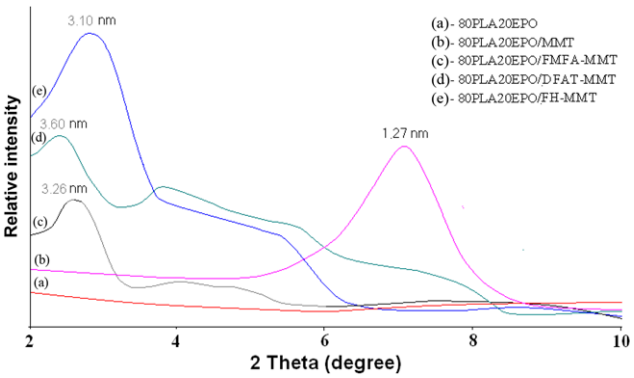

Fig. 5. XRD patterns of PLA/EPO/FNCs modified clay nanocomposites.

Table 4 Diffraction angle and basal spacing of PLA/EPO/FNCs modified clay nanocomposites

Sample	2 Theta (degree)	d-Spacing (nm)
80PLA20EPO	0.00	0.00
80PLA20EPO/MMT	6.91	1.27
80PLA20EPO/FH-MMT	2.83	3.10
80PLA20EPO/HMFA-MMT	2.64	3.26
80PLA20EPO/DFAT-MMT	2.41	3.60

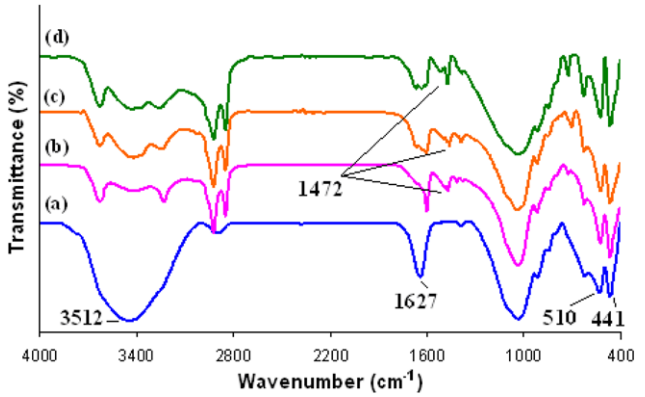

Fig. 6. FTIR spectra of (a) Na-MMT, (b) FH-MMT, (c) HMFA-MMT, and (d) DFAT-MMT.

morillonite nanocomposites. In the nanocomposites where the montmorillonite surface is pretreated with FH and HMFA, the basal spacing of the clay increased to 3.10 and 3.26 nm, respectively. However, when the montmorillonite surface is pretreated with DFAT, which has two fatty acid chains, the basal spacing further increases to 3.60 nm (Table 4). This clearly shows that the basal spacing of organoclay in the polymer matrix increases with the increase in the size of the surfactant as was observed by Agag and Takeichi [32]. These XRD patterns also suggest that all the nanocomposites produced are intercalated compounds.

The FTIR spectra of Na-MMT, FH-MMT, HMFA-MMT, and DFAT-MMT are shown in Fig. 6. In the spectra of Na-MMT, the peaks at 3,512, 1,627 and 1,009 cm^{-1} are due to the O-H stretching, interlayer water deformation and the Si-O stretching vibration, respectively. The other strong band absorption at 510 cm^{-1} and 441 cm^{-1} indicates the presence of Al-O stretching and Si-O bending, respectively, in the clay. The FH MMT, HMFA-MMT, and DFAT-MMT spectra show the major bands of FH, HMFA, and DFAT spectra [24-26] in addition to the bands of the original Na-MMT. The band at around 1,472 cm^{-1} suggests the existence of the ammonium ion. Therefore, these indicate that the FH, HMFA, and DFAT were intercalated in the silicate layers.

Elemental analysis was used to estimate the amount of FH, HMFA, and DFAT being intercalated into the clay galleries. Table 5 shows the results of N analyses of the FH, HMFA, and DFAT and the mixtures of FH, HMFA, and DFAT modified clay. The calculation is based on either carbon atoms or nitrogen atoms, because if the increase of their content is only due to the presence of the organic molecule, the calculation does not include the hydrogen content as there are possibilities of water molecules being trapped between the

Table 5. The amounts of N and alkylammonium cations of FH, HMFA, and DFAT present in the clay layers

Alkylammonium cations modified clay	%N	mmol of Alkylammonium cations/1 g clay based on atom N
FH^+	2.50	1.78
$HMFA^+$	2.73	1.94
$DFAT^+$	5.67	2.03

layers of the unmodified clay. The high contents of N in all samples indicate that alkylammonium cations were successfully exchanged into the clay. However, the %N in the unmodified clay is only 0.23%. The maximum amount of alkylammonium cations adsorbed was almost equivalent to the cation exchange capacity of the clay, indicating that the Na^+ in the clay can be easily replaced by the alkylammonium cations. The amounts of FNCs present in the organoclay were calculated by the following equation:

$$\text{Amount of FNC (mole)} = S/(100 \times A \times n) \quad (1)$$

where S=percentage of the nitrogen in the organoclay percentage of the nitrogen in the Na-MMT, A=atomic mass of nitrogen and n=number of nitrogen atoms in the FNC molecule.

Most of the thermoanalytical studies reveal new insights into the structure of intercalated clays [33]. Thermogravimetric analysis (TGA) gives information on the structure of the intercalating molecules by the weight loss steps. Thermal degradation of MMT shows two steps [34]. The first one is before 200 °C because of the volatilization of water adsorbed on the external surfaces of the MMT and water inside the interlayer space. The second step is in the range from 500-1,000 °C due to the loss of hydroxyl groups of the MMT structure. The thermal degradation of the modified MMT can be explained in four steps. The first step occurs at below 200 °C due to the vaporization of water. Decomposition of the surfactant takes place in the second step between 200-500 °C. Dehydroxylation of the aluminosilicates at the temperature range of 500-800 °C happens in the third step. In the last step, the organic carbon reacts with inorganic oxygen (combustion reaction) at about 800 °C.

The weight loss curves (TGA) of the MMT, FH-MMT, HMFA-MMT, and DFAT-MMT are illustrated in Fig. 7. MMT contains water due to hydrated sodium (Na^+) cations intercalated inside the clay layers. The presence of alkylammonium groups within the MMT interlayer spacing lowers the surface energy of the inorganic structure

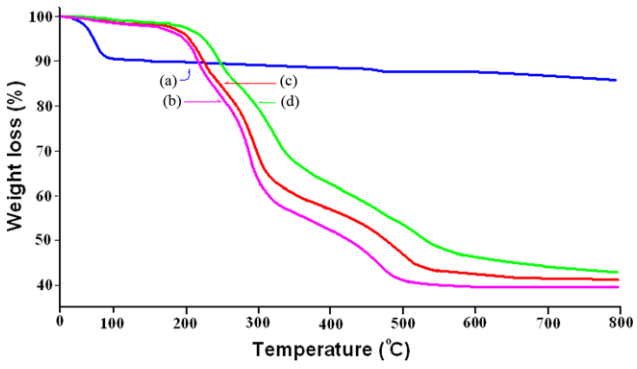

Fig. 7. TGA thermograms of (a) MMT, (b) FH-MMT, (c) HMFA-MMT, and (d) DFAT-MMT.

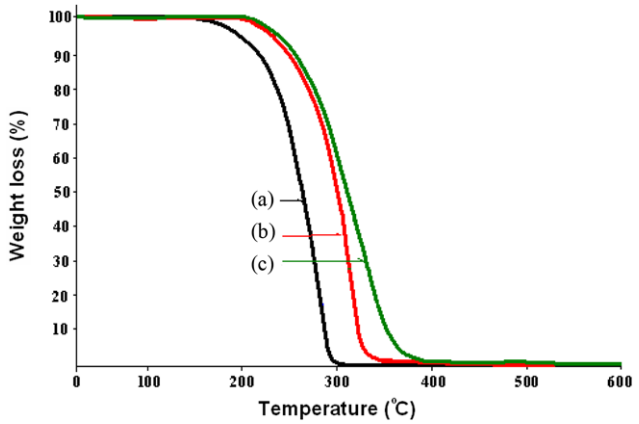

Fig. 8. TGA thermograms of (a) FH, (b) HMFA, and (c) DFAT.

and will transform organophobic to organophilic materials. The major difference between the thermogram of the unmodified clay and that of the organoclay is that the organic constituents in the organoclay decompose in the range from 200 to 500 °C, as the organic constituent in the organoclay decomposes in this range. Fig. 8 shows that the FH decomposed as the temperature increased from 158 to 600 °C. The decomposition process ended at 312 °C. The HMFA started decomposing at higher temperatures than that of the FH, which started at 192 °C and ended at 358 °C. DFAT had the highest decomposition temperature (starting at 197 °C and ending at 399 °C). It can be observed that the decomposition temperatures of the FH-MMT, HMFA-MMT and DFAT-MMT were higher than those of the pure FH, HMFA, and DFAT. The increase in the decomposition temperatures of these FNCs in the organoclays implies that there is a strong intermolecular interaction between the alkylammonium cations and the clay. In other words, after the ion exchange the FNC is intercalated and attached to the silicate layers of the clay and hence their decomposition temperatures increase.

Thermogravimetric analyses were done on PLA/EPO/FNCs-MMT nanocomposites in order to determine the effect of modified clay content in the polymer matrix on thermal properties. The results of TGA are shown in Fig. 9. The onset of the degradation of the nanocomposites is higher, that is, 283 287 and 292 °C, for PLA/EPO containing FH-MMT, HMFA-MMT, and DFAT-MMT, respectively, compared to the PLA/EPO blend (267 °C). The results show that

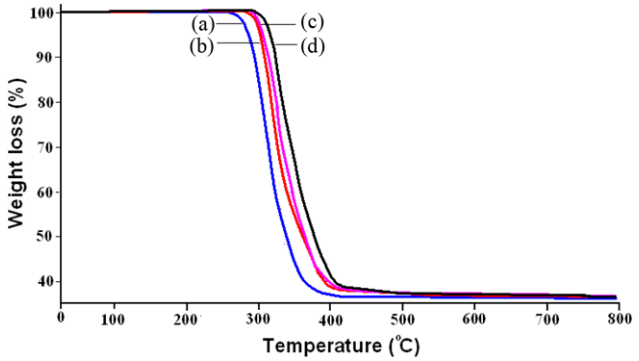

Fig. 9. TGA thermograms of (a) PLA/EPO blends, (b) PLA/EPO/FH-MMT, (c) PLA/EPO/HMFA-MMT, and (d) PLA/EPO/DFAT-MMT nanocomposites.

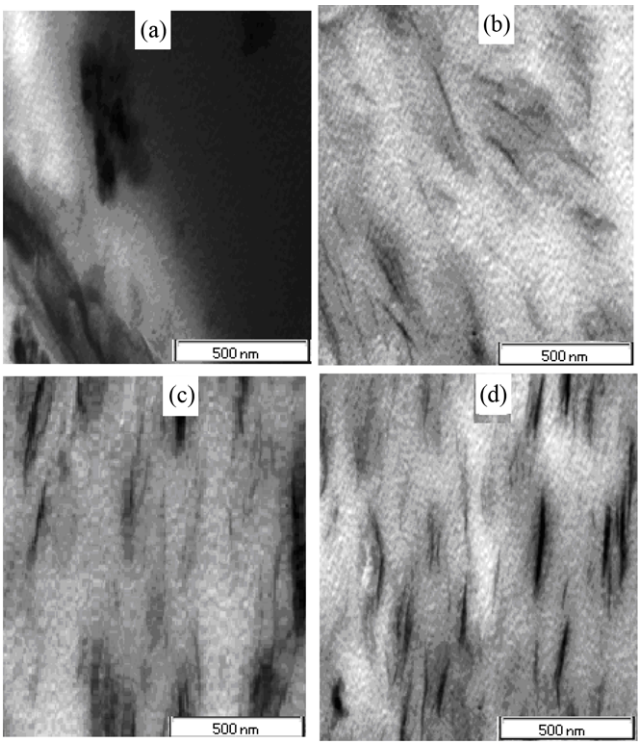

Fig. 10. TEM micrographs of (a) PLA/EPO Na-MMT, (b) PLA/EPO/DFAT-MMT, (c) PLA/EPO/FH-MMT, and (d) PLA/EPO/HMFA-MMT composites.

the thermal stability increases with addition of the FNCs. The presence of silicate layers dispersed homogeneously in the polymer sheet hinders the permeability of volatile degradation products out from the material and helps delay the degradation of the nanocomposites [35].

Figs. 10(a), (b), (c), and (d) show transmission electron microscopy (TEM) micrographs of the PLA/EPO composites reinforced with Na-MMT, DFAT-MMT, HMFA-MMT, and FH-MMT, respectively. From the PLA/EPO/Na-MMT micrograph, it can be observed that the original Na-MMT stack morphology was fully preserved with PLA/EPO due to the incompatible nature of both constituents (Fig. 10(a)). The dark lines represent the thickness of the individual clay layers or agglomerates (tactoids, stacks). The organoclay does not show its original layered structure and it is quite dispersed in the PLA/EPO matrix, especially in the presence of the PLA/EPO/FH-MMT and PLA/EPO/HMFA-MMT (Figs. 10(c) and 10(d)). The related structure can be referred to as intercalated lamellae, tactoids composed of a variable number of lamellae and aggregates of tactoids. The TEM micrograph of PLA/EPO/DFAT-MMT (Fig. 10 (b)) shows a higher degree of intercalation and some exfoliated zones. This is possibly due to the presence of two long chains of fatty acids in DFAT.

CONCLUSION

PLA/EPO clay nanocomposites have been successfully prepared by incorporating 2% DFAT-MMT and 3% of both FH-MMT and HMFA-MMT which were prepared from fatty nitrogen compounds and montmorillonite clay. TEM analysis shows that the prepared nanocomposites were of the intercalated (FH-MMT and FMFA-MMT) and partially exfoliated types (DFAT-MMT). The XRD patterns revealed that the interlayer distance of organoclays in the PLA/EPO blend was significantly increased. High thermal stability and significant improvement of mechanical properties were observed for PLA/EPO clay nanocomposites compared to PLA/EPO composites.

REFERENCES

1. Y. Lemmouchi, M. Murariu, A. Santos, A. Schacht and P. Dubois, *Eur. Polym. J*., **45**, 2839 (2009).
2. H. Tsuji and Y. Ikada. *J. Appl. Polym. Sci*., **67**, 405 (1998).
3. T. Iwata and Y. Doi, *Macromolecules*, **31**, 2461 (1998).
4. D. Sawai, K. Takahashi, T. Imamura, K. Nakamura, T. Kanamoto and S. Hyon, *Polym. Sci. Polym. Phys.*, **40**, 95 (2002).
5. M. Murariu, A. Ferreira, M. Pluta, L. Bonnaud and M. Alexandre, Duboi, *Eur. Polym. J*., **44**, 3842 (2008).
6. R. Auras, S. Singh and J. Singh, *Packag. Technol. Sci*., **18**, 207 (2005).
7. R. Auras, B. Harte, S. Selke and R. Hernandez, *J. Plastic. Film. Sheet*., **19**, 123 (2003).
8. A. Nijenhuis, E. Colstee, D. Grijpma and Pennings, *Polymer*, **37**, 5849 (1996).
9. L. Liu, S. Li, H. Garreau and M. Vert. *Biomacromol*, **1**, 350 (2000).
10. N. Lopez-Rodriguez, A. Lopez-Arraiza, E. Meaurio and J. Sarasua, *Polym. Eng. Sci*., **46**, 1299 (2006).
11. Y. Li and H. Shimizu, *Macromol. Biosci*., **7**, 921 (2007).
12. M. Baiardo, G. Frisoni, M. Scandola, M. Rimelen, D. Lips, K. Ruffieux and E. Wintermantel, *J. Appl. Polym. Sci*., **90**, 1731 (2003).
13. N. Ogata, H. Sasayama, K. Nakane and T. Ogihara, *J. Appl. Polym. Sci*., **89**, 474 (2003).
14. Z. Kulinski and E. Piorkowska, *Polymer*, **46**, 10290 (2005).
15. Z. Ren, L. Dong and Y. Yang, *J. Appl. Polym. Sci*., **101**, 1583 (2006).
16. P. LeBaron, Z. Wang and T. Pinnavaia, *Appl. Clay. Sci*., **15**, 11 (1999).
17. M. Alexandre and P. Dubois, *Mater. Sci. Eng. R. Rep*., **28**, 1 (2000).
18. A. Okada and A. Usuki, *Macromol. Mater. Eng*., **291**, 1449 (2006).
19. E. Giannelis, *Adv. Mater*., **8**, 29 (1996).
20. B. Zidelkheirl and M. Abdelgoad, *J. Therm. Anal. Cal*., **94**, 181 (2008).
21. A. Pérez-Santano, R. Trujillano, C. Belver, A. Gil and M. Vicente, *J. Colloid Interf. Sci*., **284**, 239 (2005).
22. O. Arroyo, M. Huneault, B. Favis and M. Bureau, *Polym. Compos*., **31**, 114 (2010).
23. M. Paul, M. Alexandre, P. Degée, C. Henrist, A. Rulmont and P. Dubois, *Polymer*, **44**, 443 (2003).
24. E. A. J. Al-Mulla, W. M. Z. Yunus, N. A. Ibrahim and M. Z. Abdul Rahman, *Res. J. Appl. Sci*., **3**, 545 (2008).
25. W. H. Hoidy, M. B. Ahmad, E. A. J. Al-Mulla, W. M. Z. Yunus and N. A. Ibrahim, *Orient. J. Chem*., **26**, 210 (2010).
26. W. H. Hoidy, M. B. Ahmad, E. A. J. Al-Mulla, W. M. Z. Yunus and N. A. Ibrahim, *J. Oleo Sci.*, **59**, 229 (2010).
27. ASTM D638-03, Standard test method for tensile properties of plastics (2004).
28. E. Al-Mulla, W. Yunus, N. Ibrahim and M. Rahman, *J. Mater. Sci*., **45**, 1942 (2010).
29. Y. Vu, J. Mark, L. Pham and M. Engelhardt, *J. Appl. Polym. Sci*., **82**, 1391 (2001).

30. M. Arroyo, M. Lopez-Manchado and B. Herrero, *Polymer*, **44**, 2447 (2003).
31. M. Pospisil, A. Kalcndova, P. Capkova, J. Simonik and M. Valaskova, *J. Colloid Interf. Sci.*, **227**, 154 (2004).
32. T. Agag and T. Takeichi, *Polymer*, **41**, 7083 (2000).
33. Y. Xi Y, W. Martens, H. He and R. Frost, *J. Therm. Anal. Cal*., **81**, 91 (2005).
34. M. Manchado and B. Herrero, *Polymer*, **44**, 2447 (2003).
35. S. Jamaliah, M. Wan, Z. Khairul, M. Dahlan and A. Mansor, *Polym. Test*, **24**, 211 (2005).